

## A NOTE ON THE USE OF THE GRAYLEVEL CO-OCCURRENCE MATRIX IN THRESHOLD SELECTION\*

B. CHANDA and D. Dutta MAJUMDER

Electronic and Communication Sciences Unit, Indian Statistical Institute, Calcutta 700035, India

Received 18 September 1986

Revised 13 August 1987 and 13 January 1988

**Abstract.** Graylevel thresholding is one of the most popular and economic approaches for segmentation. Graylevel co-occurrence matrices are being successfully used to measure textural properties of the image. In this report, for threshold selection we have considered four new measures based on the graylevel co-occurrence matrix, which in some way or other reflect the homogeneity in different regions of an image. They are also compared with two other measures reported already. Experimental results reveal that the newly proposed techniques are more effective for segmenting noisy images.

**Zusammenfassung.** Im Gebiet der digitalen Bildverarbeitung verwendet einer der gängigsten und ökonomischsten Ansätze zur Segmentierung Graustufen-Schwellen. "Co-occurrence"-Matrizen werden derzeit erfolgreich verwendet, um die Eigenschaften der Textur des Bildes zu messen. Im vorliegenden Bericht haben wir sechs verschiedene Maße betrachtet, die auf "co-occurrence"-Matrizen basieren und auf die eine oder andere Weise die Homogenität in verschiedenen Bereichen des Bildes widerspiegeln. Einige dieser Maße wurden bereits beschrieben und sind gut bekannt. Die übrigen werden hier vorgeschlagen und sind konzeptionell verschieden von früheren. Experimentelle Ergebnisse belegen, daß die neu vorgeschlagenen Verfahren effektiver zur Segmentierung der verrauschten Bilder sind.

**Résumé.** L'une des approches les plus populaires et économique de segmentation est le seuillage des niveaux de gris. Les matrices de co-occurrence ont eu du succès dans la mesure des propriétés texturales des images. Dans cet article, pour choisir le seuillage nous avons considéré quatre nouvelles mesures basées sur les matrices de co-occurrence de niveaux de gris qui reflètent d'une manière ou d'une autre l'homogénéité dans les différentes régions de l'image. Elles sont également comparées à deux autres mesures déjà publiées. Les résultats expérimentaux montrent que les nouvelles techniques proposées sont plus efficaces pour la segmentation des images bruitées.

**Keywords.** Image segmentation, graylevel thresholding, co-occurrence matrix.

### 1. Introduction

Scene analysis and image interpretation require images to be segmented into meaningful parts. Segmentation is basically a process of pixel classification which extracts the regions by assigning the individual pixels to classes. One of the most useful and economic technique for image segmentation is graylevel thresholding which extracts the homogeneous regions by classifying pixels based on their graylevels. The main problem of this technique is the selection of threshold. In general, the threshold is selected using the graylevel histogram. Weszka [1] has surveyed a number of threshold selection techniques using histograms. Informations provided by histograms are often found to be inadequate to select a proper threshold. In such cases, the graylevel co-occurrence matrix can be an aid to threshold selection.

\* This work is supported by D.O.E., Government of India Grant No. 3116/984 T.D.D.

The graylevel co-occurrence matrix gives an overall idea about the spatial variation of graylevel in image data. Different workers [2, 3, 4, 5] have measured different properties from this matrix for a possible threshold values. Finally, the proper threshold is selected corresponding to the optimum value of the measurement. However, the graylevel co-occurrence matrix is not the only way to compute a high dimensional histogram. The joint frequency table of other features like edge, average graylevel, Laplacian etc. with graylevel has also been employed to select thresholds [6, 7, 8]. The graylevel co-occurrence matrix has also been used in texture analysis and remote sensing applications [9, 10].

The graylevel co-occurrence matrix is defined in Section 2. Some existing measures based on this matrix are also described in this section. In this report we will study some new measures using the co-occurrence matrix and their use in threshold selection for image segmentation. Section 3 is devoted to this purpose. Section 4 describes experimental results using the approaches described in Sections 2 and 3. Finally, concluding remarks are cited in Section 5.

## 2. Some existing measures based on co-occurrence matrix

Let the discrete variable  $m$  represent the graylevel of pixel  $(j, k)$  and the discrete variable  $n$  represent the graylevel of pixel  $(j-d \sin \theta, k+d \cos \theta)$  of a  $L$ -level graytone image  $[g]$ , i.e.  $[g] = \{g(j, k) | j=0, 1, 2, \dots, M-1, k=0, 1, 2, \dots, N-1\}$  and  $m, n=0, 1, 2, \dots, L-1$ . We are interested in considering the co-occurrence of graylevels in pairs of pixels where one is lying at a distance of  $d$  in the direction  $\theta$  with respect to the other. Here we take the value of  $d$  equal to 1 and  $\theta$  as an integer multiple of  $\frac{1}{2}\pi$ .

Now the elements of the graylevel co-occurrence matrix  $[C_\theta]$  for the direction  $\theta$  can be defined as

$$c_{m,n,\theta} = \sum_{j=0}^{M-1} \sum_{k=0}^{N-1} \# \{g(j, k) = m \wedge g(j-d \sin \theta, k+d \cos \theta) = n\}, \quad (1)$$

where,  $\# \{ \cdot \}$  is equal to 1 if the argument is true and is equal to 0 if the argument is false. The element  $c_{m,n,\theta}$  gives the frequency that a pixel having graylevel  $n$  occurs adjacent to a pixel having graylevel  $m$  in the direction  $\theta$ . Considering all the directions, the co-occurrence matrix is obtained as

$$[C] = \{c_{m,n}\} = \frac{1}{2} \{([C_\theta] + [C_{\theta+\pi}] + [C_{\theta+\frac{\pi}{2}}] + [C_{\theta+\frac{3\pi}{2}}])\}. \quad (2)$$

Since  $[C_\theta] = [C_\theta]^T$  and  $[C_{\theta+\pi}] = [C_{\theta+\pi}]^T$ , hence eq. (2) can be simplified to

$$[C] = \frac{1}{2} \{([C_\theta] + [C_\theta]^T + [C_{\theta+\frac{\pi}{2}}] + [C_{\theta+\frac{\pi}{2}}]^T)\}.$$

So  $[C]$  is a symmetric matrix of size  $L \times L$  and its elements are nonnegative, i.e.,

$$c_{m,n} = c_{n,m} \quad \text{and} \quad c_{m,n} \geq 0.$$

For simplicity let us assume  $g(j, N) = g(j, 0)$ ,

$$g(j-1) = g(j, N-1), \quad g(M, k) = g(0, k) \quad \text{and} \quad g(-1, k) = g(M-1, k).$$

Then

$$\sum_{n=0}^{L-1} c_{m,n} = \sum_{n=0}^{L-1} c_{n,m} = h_m(i), \quad (3)$$

$h_m(i)$  is the  $i$ th entry of the graylevel histogram of the image, since both  $m$  and  $n$  represent the same physical quantity, i.e., the graylevel present in the image.

Let  $t$  be the graylevel threshold that maps the original image into two distinct sets of regions  $R_1$  and  $R_2$ . This mapping consequently divides the graylevel co-occurrence matrix into four nonoverlapping blocks as shown in Fig. 1.

The respective blocks of  $[C]$  represent

- the co-occurrence of graylevel in region  $R_1$ , say, i.e., those  $c_{m,n}$  for which  $m \leq t$  and  $n \leq t$  (shaded area  $B_1$ ),
- the co-occurrence of graylevel in region  $R_2$ , i.e., those  $c_{m,n}$  for which  $m > t$  and  $n > t$  (shaded area  $B_4$ ), and
- the co-occurrence of graylevels in the border region of  $R_1$  and  $R_2$ , i.e., those  $c_{m,n}$  for which either  $m \leq t$  and  $n > t$  (shaded area  $B_2$ ) or  $m > t$  and  $n \leq t$  (shaded area  $B_3$ ).

The methods of threshold selection using the co-occurrence matrix can be divided into two classes. One looks, directly or indirectly, for the threshold for which the number of pairs of border pixels, i.e., sum of  $c_{m,n}$  over the blocks  $B_2$  and  $B_3$  of Fig. 1, is minimal. In other words, it searches for a threshold which segments the image into the largest homogeneous regions possible. Measures like *Busyness* [3], *conditional probability* [4] and *entropy* belong to this class.

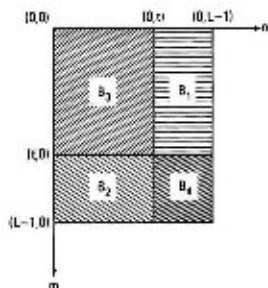


Fig. 1. Four non-overlapping blocks of graylevel co-occurrence matrix, where  $t$  is value of threshold.

**Busyness measure.** The Busyness measure [3] for the threshold  $t$  can be defined as

$$\text{Busyness}(t) = \sum_{m=0}^{t-1} \sum_{n=t}^{L-1} c_{m,n} + \sum_{m=t}^{L-1} \sum_{n=0}^{t-1} c_{m,n} \quad (4)$$

for  $t = 0, 1, 2, \dots, L-2$ . The method for selecting the threshold is as follows.

Search for minima in  $\text{Busyness}(t)$ . Select the value of  $t$  as the threshold which corresponds to minimum among these minima, if the image contains only two types of regions. If the image contains more than two types of regions, then every value of  $t$  corresponding to every minimum is taken as the distinct threshold.

Equation (4) can also be written as

$$\text{Busyness}(t) = MN - \left( \sum_{m=0}^{t-1} \sum_{n=0}^{t-1} c_{m,n} + \sum_{m=t}^{L-1} \sum_{n=t}^{L-1} c_{m,n} \right), \quad (5)$$

for  $t = 0, 1, 2, \dots, L-2$ . For the acceptable threshold, for which the Busyness measure is minimum among minima, the portion within parentheses on the right hand side of equation (5) which gives the total number of pixels in region  $R_1$  and  $R_2$ , respectively is maximum among maxima. That means the threshold segments the image into the largest homogeneous region possible. So the method is useful for segmenting image which consist of large smooth regions.

Again, the computational cost for the Busyness measure can be reduced by using the following recurrence relationship.

$$\begin{aligned} \text{Busy}(0) &= 2 \sum_{n=0}^{L-1} c_{0,n} \\ \text{Busy}(t) &= \text{Busy}(t-1) + 2 \left[ \sum_{k=t+1}^{L-1} c_{k,t} - \sum_{n=0}^{t-1} c_{n,t} \right], \\ &\text{for } t = 1, 2, 3, \dots, L-2. \end{aligned}$$

**Conditional probability.** Deravi and Pal [4] measured the probability of pixel  $(j - \sin \theta, k + \cos \theta)$  lying in  $R_2$  when  $(j, k)$  is known to lie in  $R_1$ , and of pixel  $(j - \sin \theta, k + \cos \theta)$  lying in  $R_1$  when  $(j, k)$  is known to lie in  $R_2$ . So this conditional probability for a threshold  $t$  may be expressed as

$$\begin{aligned} \text{Cond. prob.}(t) &= \frac{\text{Pr}\{g(j - \sin \theta, k + \cos \theta) > t, g(j, k) \leq t\}}{\text{Pr}\{g(j, k) \leq t\}} \\ &+ \frac{\text{Pr}\{g(j - \sin \theta, k + \cos \theta) \leq t, g(j, k) > t\}}{\text{Pr}\{g(j, k) > t\}} \\ &= \frac{\text{Pr}\{g(j - \sin \theta, k + \cos \theta) > t, g(j, k) \leq t\}}{\text{Pr}\{g(j, k) \leq t\}} \\ &+ \frac{\text{Pr}\{g(j - \sin \theta, k + \cos \theta) \leq t, g(j, k) > t\}}{\text{Pr}\{g(j, k) > t\}}. \end{aligned}$$

Hence, from the co-occurrence matrix we can write

$$\text{Cond. prob.}(t) = \frac{\sum_{n=0}^t \sum_{k=t+1}^{L-1} P_{n,t}}{\sum_{n=0}^t \sum_{k=0}^{L-1} P_{n,t}} + \frac{\sum_{n=t+1}^{L-1} \sum_{k=0}^t P_{n,t}}{\sum_{n=t+1}^{L-1} \sum_{k=0}^{L-1} P_{n,t}}, \quad (6)$$

for  $t = 0, 1, 2, \dots, L-2$ , where  $P_{n,t} = c_{n,t} / MN$ .

Simplifying equation (6) we obtain

$$\text{Cond. prob.}(t) = \frac{MN \text{ Busy}(t)}{2 \left[ \sum_{i=0}^t h_1(i) \right] \left[ MN - \sum_{i=0}^t h_2(i) \right]} \quad (7)$$

For this measure also a recurrence relationship similar to that for Busyness measure can be established.

However, for the image consisting of large homogeneous regions, the probability of pairs of pixels of which one is lying in  $R_1$  and other in  $R_2$ , i.e., the probability of border pairs is less. So in this case also the threshold is selected in a similar way as in the case of the Busyness measure and a satisfactory result for some images can be achieved.

### 3. Some new measures of image properties

In the previous section both the measures actually compute the probability (in a very crude sense) of the pixels lying on the border regions. Here we suggest some new measures describing other properties such as entropy, contrast etc. of the image and select the threshold accordingly.

**Entropy measure.** Both measures described above, directly or indirectly, count the pairs of border pixels. Here is another measure, namely the entropy or information content of border pixels, of a similar category and which is defined as

$$\text{Entropy}(t) = - \sum_{m=0}^t \sum_{n=t+1}^{L-1} p_{m,n} \log p_{m,n} - \sum_{m=t+1}^{L-1} \sum_{n=0}^t p_{m,n} \log p_{m,n} \quad (8)$$

$$\text{for } t = 0, 1, 2, \dots, L-2.$$

Since  $\log p_{m,n}$  is a monotonic increasing function of  $p_{m,n}$ , the approach to select a graylevel threshold is similar to that using the Busyness measure. But the present measure has an advantage in that it takes care of the distribution  $p_{m,n}$  (or  $c_{m,n}/MN$ ) over areas  $B_1$  and  $B_2$  of Fig. 1 unlike Busyness measure which consider only aggregates of  $c_{m,n}$  over these areas. To reduce the computational cost the following recurrence relationship can be used.

$$\text{Entropy}(0) = -2 \sum_{m=1}^{L-1} p_{0,m} \log p_{0,m}$$

$$\text{Entropy}(t) = \text{Entropy}(t-1) + 2 \left[ \sum_{m=0}^{t-1} p_{m,t} \log p_{m,t} - \sum_{m=t+1}^{L-1} p_{m,t} \log p_{m,t} \right]$$

$$\text{for } t = 1, 2, 3, \dots, L-2.$$

The other class of methods for threshold selection defines a suitable function of  $c_{m,n}$  and then looks for the threshold for which the function attains an optimum value. Measures like average contrast [5], Weber contrast and average entropy belong to this class.

**Average contrast measure.** It is known that, in an image, contrast is maximum at the regions where different types of regions meet. So those  $c_{m,n}$ , where pixel having graylevel  $m$  and pixel having graylevel  $n$  lie in different types of regions, are responsible for the maximum contrast and the magnitude of contrast is an even function of difference in graylevels, i.e.,  $(m-n)$ . Average contrast per pixel in the border region for the threshold  $t$  can be defined as [5].

$$\text{Av. cont.}(t) = \frac{\sum_{m=0}^t \sum_{n=t+1}^{L-1} (m-n)^2 c_{m,n}}{\sum_{m=0}^t \sum_{n=t+1}^{L-1} c_{m,n}} + \frac{\sum_{m=t+1}^{L-1} \sum_{n=0}^t (m-n)^2 c_{m,n}}{\sum_{m=t+1}^{L-1} \sum_{n=0}^t c_{m,n}} \quad (9)$$

$$\text{for } t = 0, 1, 2, \dots, L-2.$$

Equation (9) can be simplified to

$$\text{Av. cont.}(t) = \frac{\sum_{m=t+1}^{L-1} \sum_{n=0}^t (m-n)^2 c_{m,n}}{\text{Busy}(t)}, \quad (10)$$

The method for selecting the threshold based on this measure is as follows. Search for maxima in  $Av. cont.(t)$ . Select the value of  $t$  as threshold which corresponds to the maximum among these maxima, if the image contains only two types of regions. If the image contains more than two types of regions, then every value of  $t$  corresponding to every maximum is taken as a distinct threshold.

Equation (10) reveals that the maximum among maxima found in  $Av. cont.(t)$  may not correspond to the minimum among minima found in  $Busy(t)$ . So this method of threshold selection is conceptually different from those described earlier.

**Weber contrast measure.** Average contrast of an image can also be defined incorporating human visual response, specifically logarithmic response to brightness (Weber's law). Here, instead of squared difference of graylevels, contrast is defined as the ratio of the difference of graylevels of neighbouring pixels to the minimum of them. Then the average contrast, we call it here Weber contrast, is given as

$$Web. cont.(t) = \frac{\sum_{m=0}^{L-1} \sum_{n=t+1}^{L-1} \frac{|m-n|}{\min(m,n)} c_{m,n}}{\sum_{m=0}^{L-1} \sum_{n=t+1}^{L-1} c_{m,n}} + \frac{\sum_{m=t+1}^{L-1} \sum_{n=0}^{t-1} \frac{|m-n|}{\min(m,n)} c_{m,n}}{\sum_{m=t+1}^{L-1} \sum_{n=0}^{t-1} c_{m,n}} \quad (11)$$

for  $t=0, 1, 2, \dots, L-2$ . The expression can be simplified (from a computational point of view) to

$$Web. cont.(t) = \frac{\sum_{m=0}^{L-1} \frac{1}{m} \sum_{n=t+1}^{L-1} (n-m) c_{m,n}}{Busy(t)} \quad (12)$$

During the calculation of this measure we shift the graylevel range from  $[0, L-1]$  to  $[1, L]$ , to avoid division by zero.

The method for selecting the threshold based on this measure is the same as that for the average contrast measure.

**Average entropy measure.** It is observed that edge points play the most important role in detecting and interpreting an object in an image by a human observer. So one may argue that average entropy per pixel in the border region should be maximum. Average entropy per pixel for a threshold  $t$  may be defined as

$$Av. ent.(t) = \frac{\sum_{m=0}^{t-1} \sum_{n=t+1}^{L-1} p_{m,n} \log p_{m,n} + \sum_{m=t+1}^{L-1} \sum_{n=0}^{t-1} p_{m,n} \log p_{m,n}}{\sum_{m=0}^{t-1} \sum_{n=t+1}^{L-1} c_{m,n} + \sum_{m=t+1}^{L-1} \sum_{n=0}^{t-1} c_{m,n}} \quad (13)$$

for  $t=0, 1, 2, \dots, L-2$ .

Since  $[C]$  is a symmetric matrix, equation (13) can be simplified to

$$Av. ent.(t) = \frac{Entropy(t)}{Busy(t)} \quad (14)$$

Equation (14) reveals that, to reduce computational cost, a recurrence relationship for average entropy measure can be found. The approach to select the graylevel threshold is similar to that using average contrast.

#### 4. Experimental results

The threshold selection techniques described above using graylevel co-occurrence matrix are tested on several images. The thresholds selected automatically using different measures are used to segment three different images. In our experiment we have used both types of images, namely images consisting of two types of regions and images consisting of more than two types of regions. Here we will show the results of implementation of the segmentation algorithm at least on one image from each class. Images are sampled into  $64 \times 64$  pixels resolution and intensity values are quantized into 32 levels.

First, we consider Fig. 2(a)i which is a microphotograph of 'chromosomes'. The image contains only two types of regions, namely chromosomes (objects) and background. Fig. 2(a)ii shows the graylevel histogram of this image and reveals that being nearly unimodal it is not trivial to detect a threshold using this histogram.

Figs. 2(b-g)ii exhibit plots of different measures, namely Busyness, conditional probability, entropy, average contrast, average entropy and Weber contrast, respectively, versus graylevel (or all possible values of threshold). Segmented images using thresholds selected from these measures are shown in Figs. ii correspondingly.

The result shown in Fig. 2(e)ii, in this case, is best, followed by that shown in Fig. 2(f)ii and Fig. 2(g)ii, respectively. Results shown in Figs. 2(b)ii, 2(c)ii and 2(d)ii are not satisfactory. For example, in those images a considerable area of background is included in the top-left hand 'chromosome' as its part. Plots of Busyness measure and entropy measure [i.e., Figs. 2(b)ii and 2(d)ii] are almost similar. However, all three measures: busyness, cond. prob. and entropy have led to the same result.

The second image we have chosen, for our experiment, to show performances of different measures is shown in Fig. 3(a)i. Fig. 3(a)ii shows its graylevel histogram. This image of 'cells' consists of three types of regions, namely nucleus, cytoplasm and background.

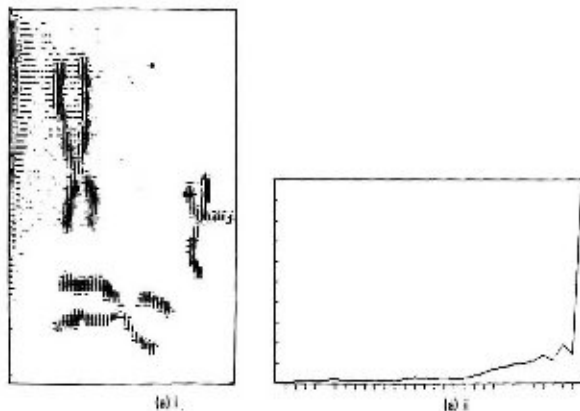


Fig. 2(a) i, Original image of 'chromosomes' where graylevel varies from 0 to 31; ii, graylevel histogram of (a)i.

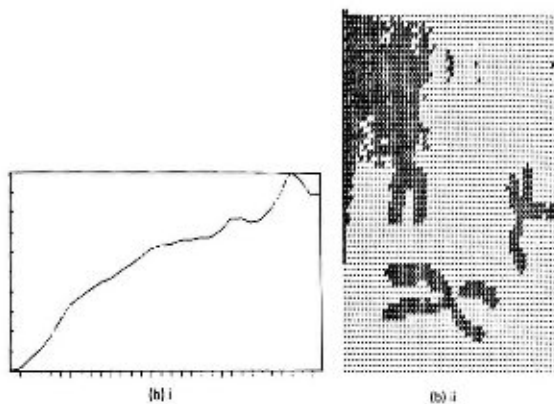


Fig. 2(b) i, Plot of Bayes measure versus threshold; ii, segmented image using threshold detected from (b).

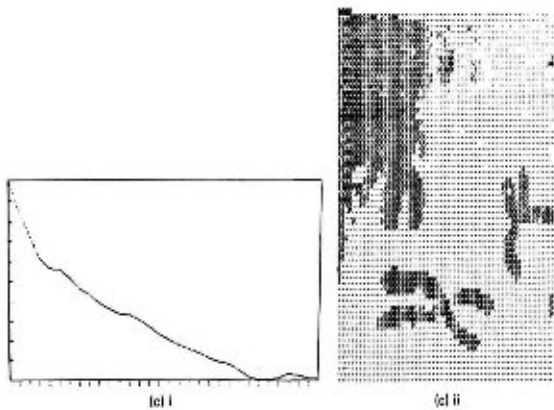


Fig. 2(c) i, Plot of conditional probability measure versus threshold; ii, segmented image using threshold detected from (c).



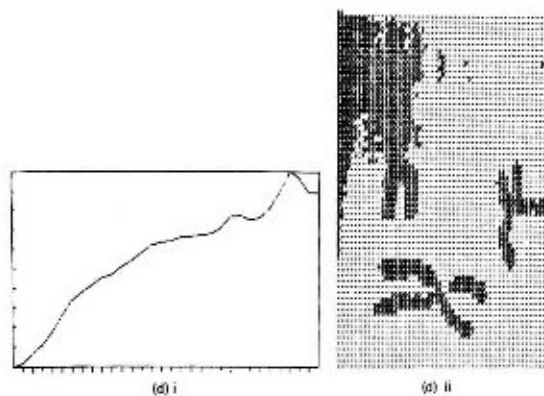


Fig. 2(d) i, Plot of entropy measure versus threshold; ii, segmented image using threshold detected from (d) i.

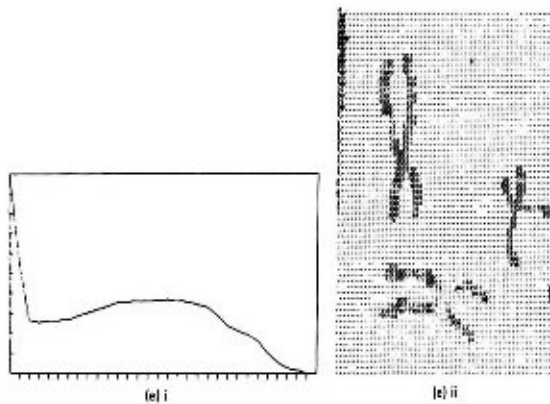


Fig. 2(e) i, Plot of average contrast versus threshold; ii, segmented image using threshold detected from (e) i.

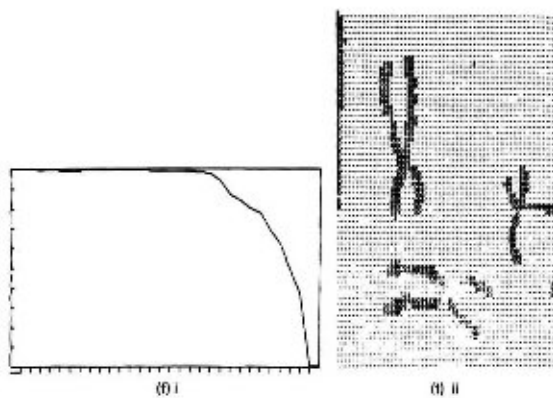


Fig. 2: i, Plot of average entropy versus threshold; ii, segmented image using threshold derived from (i).

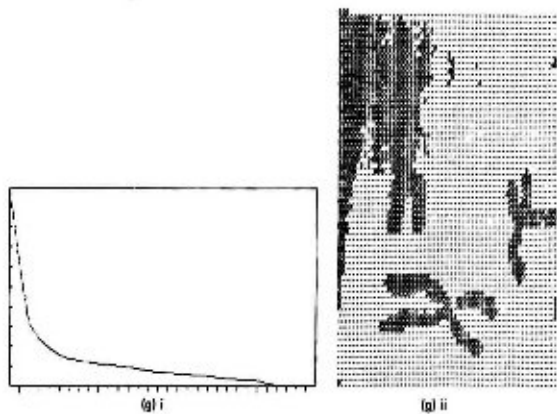


Fig. 3: i, Plot of Weber contrast versus threshold; ii, segmented image using threshold derived from (i).

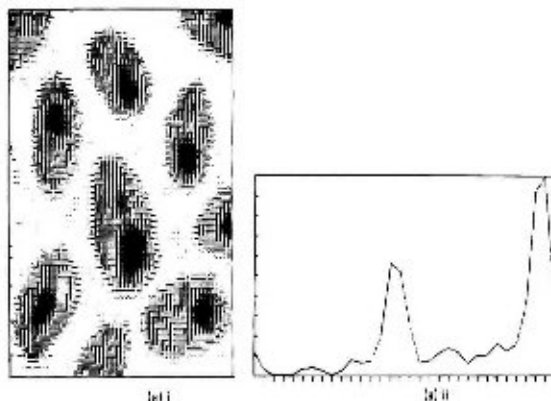


Fig. 3(a) i, Original image of 'cell' where graylevel varies from 0 to 255; ii, gray level histogram of (a) i

Figures 3(b)–g)ii exhibit plots of different measures versus graylevel and corresponding figures, i.e., Figs. 3(b)–g)iii show the segmented images using thresholds selected from the respective plot. The result shown in Fig. 3(e)iii is the best in this case, since all the three regions are detected with desired shape. This result is followed by Fig. 3(g)iii and Fig. 3(f)iii, respectively, in the order of merit. A fourth region is detected in Fig. e(f)iii where cytoplasm and background meet. This particular region is also visible in Figs. 3(c)iii and Fig. 3(d)iii. However, in the former figure the nucleus is detected with larger shape and in the latter the nucleus is absent. As we have said earlier, plots of Busyness measure and entropy measure look almost similar. However, the former measure is capable of detecting only two thresholds in this case, unlike the latter one which detects three different thresholds leading to four segmented regions.

Figure 4(a)ii is an image of the planet Saturn and Fig. 4(a)iii shows its graylevel histogram. The image is assumed to contain only two regions. Fig. 4(b)–g)ii represent the various measures versus graylevel threshold and Fig. 4(b)–g)iii, as before, the corresponding segmented images. The results reveal that Fig. 4(g)iii is best in this case followed by Figs. 4(c)iii and 4(e)iii, respectively. Though the plots of Busyness measure and entropy measure look almost similar; the threshold selected due to latter measure has classified more object pixels to the backgrounds. However, results due to entropy measure and average entropy measure, i.e., Figs. 4(d)iii and 4(f)iii are almost the same.

## 5. Conclusion

In this report we have proposed four different measures using graylevel co-occurrence matrix for threshold selection. These are: entropy, average contrast, average entropy and Weber contrast. Their performances are compared with those of two well-known measures, namely Busyness and conditional

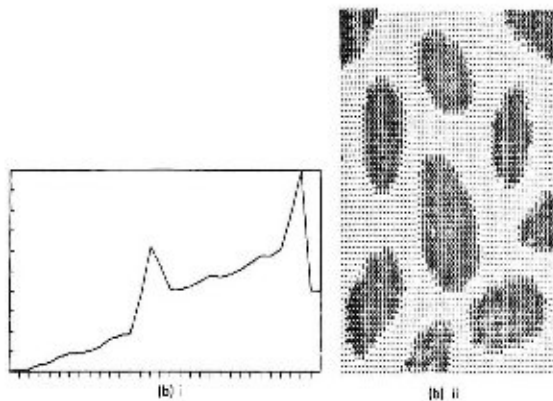


Fig. 3(b) (i) Plot of Bayes measure versus threshold; (ii) segmented image using threshold detected from (i).

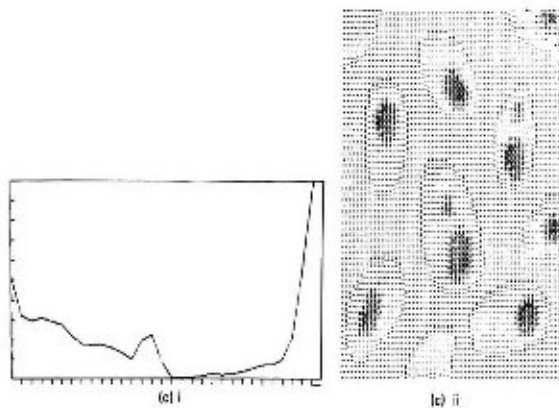


Fig. 3(c) (i) Plot of conditional probability measure versus threshold; (ii) segmented image using threshold detected from (i).

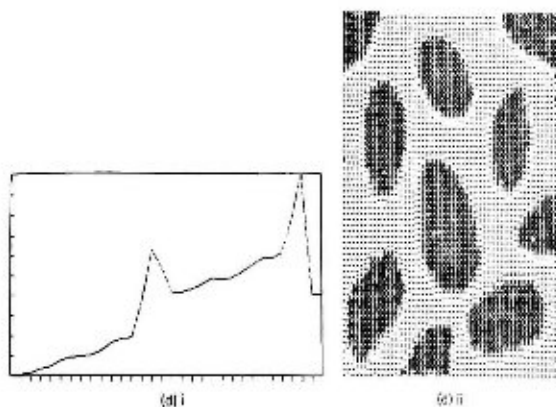


Fig. 1(d) i, Plot of entropy measure versus threshold; ii, segmented image using threshold detected from (d) i.

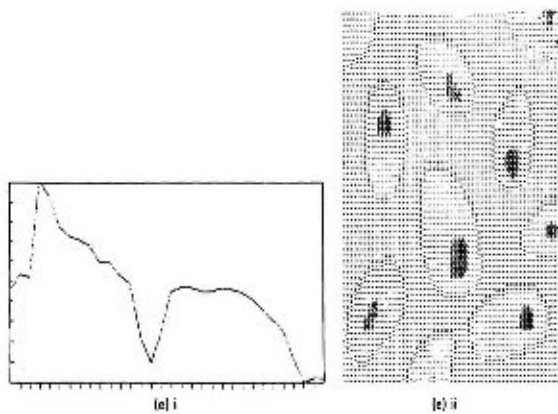


Fig. 1(e) i, Plot of average contrast versus threshold; ii, segmented image using threshold detected from (e) i.

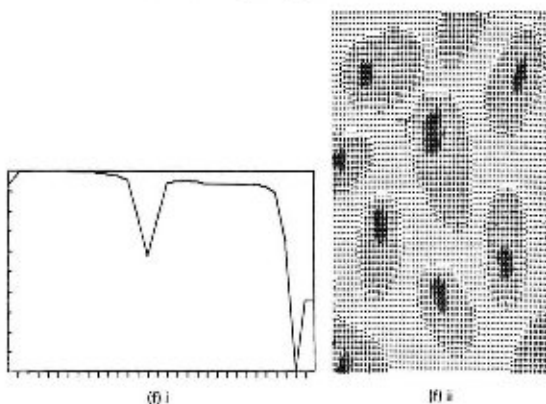


Fig. 3(i) – Plot of average entropy versus threshold; (ii) segmented image using threshold derived from (i).

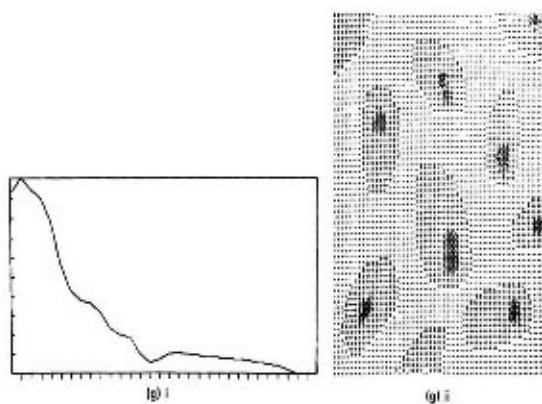


Fig. 3(i) – Plot of Weber contrast versus threshold; (ii) segmented image using threshold derived from (i).

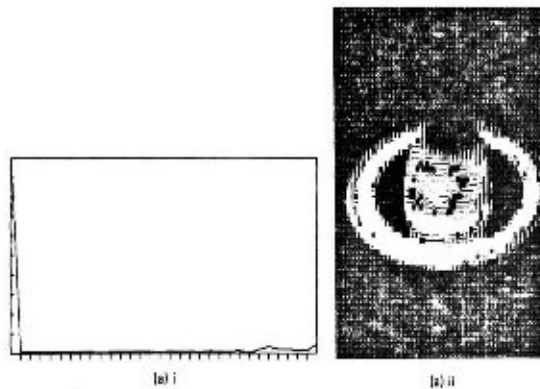


Fig 4(a) i, Original image of planet 'Saturn' where grayscale varies from 0 to 255, ii, a 4-level histogram of (a) i.

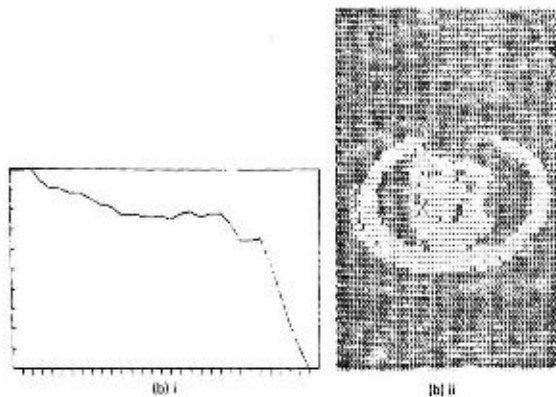


Fig 4(b) i, Plot of Otsu's measure versus threshold; ii, segmented image using threshold detected from (b) i.

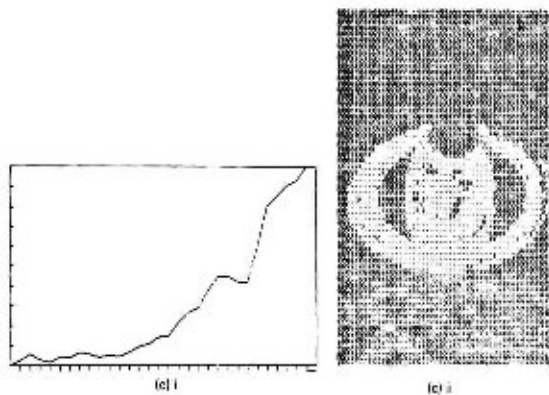


Fig. 4(c) i, Plot of conditional probability measure versus threshold; ii, segmented image using threshold-based method

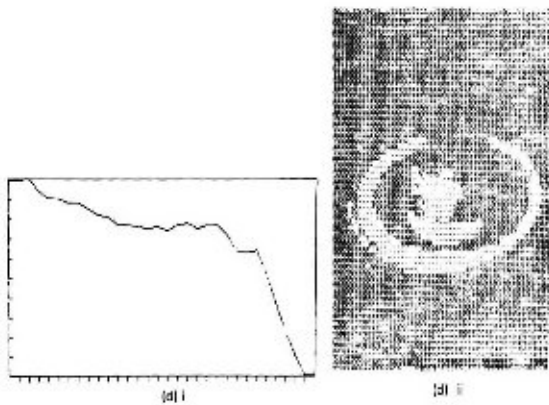


Fig. 4(d) i, Plot of entropy measure versus threshold; ii, segmented image using threshold-based method



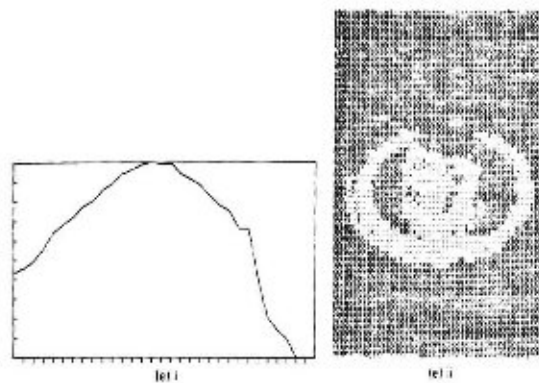


Fig. 4(e) i, Plot of average contrast versus threshold; ii, segmented image using threshold detected from (e) i.

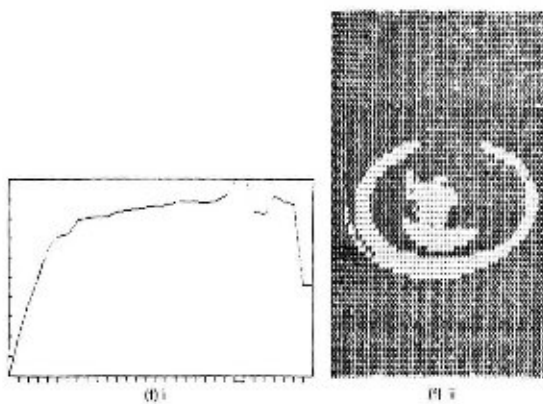


Fig. 4(f) i, Plot of average entropy versus threshold; ii, segmented image using threshold detected from (f) i.

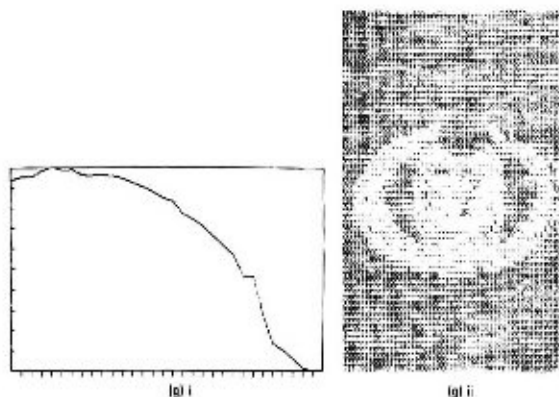


Fig. 4. (i) Plot of Weber contrast versus threshold, (ii) segmented image using threshold selected from (i).

probability. For a noise-free good quality image, performances of all the measures are found to be comparable. But for real-world images which are degraded and noisy, the results obtained by using the average contrast measure are most reliable. The result of the average entropy measure is nearest to them. Results obtained by using the conditional probability measure and the entropy measure are seen to be comparable and are worse than the previous measures. Another point is to note that the plots of the entropy measure and the Busyness measure are almost similar, the performance of the latter is worst of all. However, we must conclude with the statement that the comparisons given here are based on our experiments and it is not wise to draw any general inference about their performances.

#### Acknowledgment

Authors like to express their thanks to Mrs. S. De Bhowmick for typing the manuscript.

#### References

- [1] J.S. Wazha, "A survey of threshold selection technique", *CGIP*, Vol. 7, 1978, pp. 258-265.
- [2] R.M. Haralick, "Textural features for images classification", *IEEE Trans. SMC*, Vol. SMC-3, 1973, pp. 610-621.
- [3] J.S. Wazha and A. Rosenfeld, "Threshold evaluation techniques", *IEEE Trans. SMC*, Vol. SMC-8, 1978, pp. 622-625.
- [4] F. Dorezi and S.K. Pal, "Generalized thresholding using second order statistics", *PRL*, Vol. 1, 1983, pp. 47-49.
- [5] B. Chandra, B.B. Chaudhuri and D. Datta Majumdar, "Image enhancement and threshold selection technique using the gray-level co-occurrence matrix", *PRL*, Vol. 1, 1985, pp. 243-251.
- [6] S. Watanabe, "An automated cancer prognosis apparatus", *CYBERNETICS*, *CGIP*, Vol. 3, 1974.

- [7] J. Kittler, J. Illingworth, J. Fogelin and K. Psier, "An automatic thresholding algorithm and its performance," *Proc. 7th Internat. Conf. on Pat. Rec., Montreal, 1984*, pp. 287-295.
- [8] R. Kohler, "A segmentation system based on thresholding", *CGIP*, Vol. 15, 1981, pp. 319-334.
- [9] R.W. Coates, M.M. Trivedi and C.A. Harlow, "Segmentation of a high-resolution urban scene using texture operators," *CGIP*, Vol. 25, 1984, pp. 273-310.
- [10] R.M. Haralick and K.S. Shanmugan, "Combined spectral and spatial processing of ERTS imagery data", *Remote Sensing of Environment*, Vol. 3, 1974, pp. 3-11.